

Development of cardiac phantom which mimics the heart function using a 4.7t preclinical MRI system for cardiac imaging

Eze BE ^{1,*}, Ettah EB ¹, Ushie, PO ¹, Bassey AE ² and Igomah GO ³

¹ Department of Physics, Cross River University of Technology, Calabar, Nigeria.

² Department of Sociology (Medical), University of Calabar, Calabar, Nigeria.

³ Department of Physics, University of Calabar, Calabar, Nigeria.

World Journal of Advanced Research and Reviews, 2023, 18(03), 256–263

Publication history: Received on 22 April 2023; revised on 02 June 2023; accepted on 04 June 2023

Article DOI: <https://doi.org/10.30574/wjarr.2023.18.3.0463>

Abstract

Cardiac MRI was one of the first MRI applications in the 1980s, which helps in the human study of different cardiovascular diseases. MRI is a noninvasive imaging technique that can be used for diagnosis and has advantages over other imaging techniques since it does not rely on radiation like X-rays, PET, and SPECT. Modern clinical methods do not require much scanning time, it reveals good contrast between tissues and can compensate for patient movement during the scan. The scanner used is a 300mm internal diameter superconducting magnet (Magnex Uk) 4.7T preclinical MRI system, in the Biomedical Physics building at the University of Aberdeen. The cardiac phantom is made of a balloon filled with water, connected via a nylon T-piece to two 5 m lengths of rigid pvc tubing of 3 mm internal diameter to a 12 V water pump and solenoid valve located outside the 4.7 T MRI system's 5 Gauss stray field contour. The balloon part of the phantom was fixed on the 4.7 T MRI system's animal bed, directly over a 30mm diameter surface coil normally used to image the rat heart. The flow system was primed with water to mimic blood and the bed was loaded into the MRI magnet for imaging. The cardiac phantom has successfully been developed using a small balloon to represent a heart chamber and imaged in a 4.7T preclinical MRI scanner. Images acquired with gradient echo pulse sequence with shorter TE of 5 ms and using surface coil displayed improved image contrast and have useful signal-to-noise ratio as compared to images acquired with birdcage coil which show ghosting artifact.

Keywords: Cardiac phantom; Heart function; Cardiac imaging; Balloon phantom; 4.7T MRI; Heart chamber; Preclinical MRI.

1. Introduction

Cardiovascular diseases are one of the leading causes of death globally, the most common ones are atherosclerotic coronary artery disease and ischemic heart disease. Coronary artery disease leads to over 80% of sudden cardiac death, which occurs within 24 hours of the onset previous from patients with asymptomatic. **Bartling, et al, (2010)**.

Myocardial Infarction (MI) also known as a heart attack occurs due to a prolonged lack of blood flow to the coronary muscle resulting in some cell death, depending on the time at which blood occluded. Thrombosis is a common cause of blood clotting, arising from coronary arterial narrowing by atherosclerotic. Coronary bypass surgery is one of the treatment methods for cases associated with myocardial infarction, using healthy vessels, and enzymes to break down clots **Bartling, et al, (2010)**.

Animal models of human cardiovascular disease are mostly used since they are readily available and have aided the need to translate MRI (techniques) for clinical to preclinical laboratory and are useful in cardiac research Vallee, et al

* Corresponding author: Eze, B.E.

(2004). The reason why the main parameters of interest are the respiration rate, the temperature, and the ECG, is because the animal model is used as a laboratory experiment for human disease. There is a very close relationship between humans and small rodents (mice and rats), in terms of their respiration rates, temperature rates, and ECG. The temperature of a human being is 37°C, while that of mice and rats is 36.9°C and 37.5°C respectively. The respiratory rates of mice and rats are higher than that of humans. Also, their heartbeat increases with age but, of humans decrease with age. The heartbeat of mice ranges from 400-600 beat per minute and that of rats is from 250-400 bpm, **Brown et al**,(1999). Their respiratory rates are 163 beats per minute for mice and 85 bpm for rats, then humans' heartbeat is from 60-80bpm and respiratory rates of 12-20bpm for adult humans at rest. Also, the time of blood circulation for rats and mice are short, which is around 10 seconds while for humans is about 30 seconds. Their blood systolic pressure is also closely related, the systolic pressure of mice is from 83-164 mmHg, for rats is from 50-70mmHg, and that of humans is from 80-120mmHg **Riches, et al, (2009)**.

More studies of small animals (rat and mouse) in preclinical MRI designed to assess new techniques it has also aided the need for the development of cardiac phantom which mimics some behaviors of heart tissues to provide test data **Cardiovasc, et al, (2006)**.

Cardiac MRI was one of the first applications in the 1980s, which helps in the human study of different cardiovascular diseases. MRI is a noninvasive imaging technique that can be used for diagnosis and has advantages over other imaging techniques since it does not rely on radiation like X-rays, PET, and SPECT. Modern clinical methods do not require much scanning time, it reveals good contrast between tissues and can compensate for patient movement during scans **Fortune, et al, (2012)**.

The Heart is the major transport system of the body which pumps blood to organs and transports oxygen, nutrients, immune agents, waste products, and hormones to and from tissues. The heart is located between the lungs, fist-sized double pump, and the pumps consist of four chambers right and left atria and left and right ventricles. The right atrium links the right ventricle by the tricuspid valve, these valves prevent the backward flow of blood into the atrium, while the left atrium links the left ventricle by the bicuspid valve which prevents the backflow of blood to the atrium. Cardiac muscle cells known as myocardium allow the heart to contract and pump blood through more tissues when the left ventricular myocardium thickens. The amount of blood that flows/is pumped by the left ventricle of the heart in a single contraction (stroke volume) is 70mL in a healthy man, the heart pumps about 5L/min or greater than 30L/min during exercise, **Bartling, et al, (2010), Brown, et al, (1999)**.

The pumping action of the heart chambers is timed by waves of electrical activity flowing along specialized conduction fibers. Electrical events of the heart at any time can be detected by measuring potential differences between pairs of electrodes placed on the surface of the body which detects small voltage due to the sum of action potential in cardiac muscle. A typical Electrocardiogram (ECG) trace indicates the cardiac event **Hermann, et al, (2014)**.

It is important to monitor animal temperature rate, respiration rate, heartbeat, and ECG during physiological signal acquisition, because of animal welfare, and, also to generate respiratory and ECG signals. The biological motion from cardiac, and respiratory activities of the animal during signal acquisition is the main challenge for in vivo imaging, these motions have a great effect on the image quality. Contrary to humans that can be asked to hold their breath during signal acquisition, small animals have to be anesthetized, which will help to control their movement during imaging. But their respiratory and cardiac motion still needs to be controlled, and they usually breathe freely which can cause motion artifacts in the images **Hermann, et al, (2014)**.

The main aim of this project is to design a cardiac phantom that mimics the dynamic behavior of a rodent heart suitable for MRI and provides realistic MRI data, in left ventricular and motion in short axis view. The phantom has a general dimension of a typical mouse and changes in wall thickness, also mimicking ventricular blood flow during motion. A typical mouse has around 1.4 mL of total blood volume and a body weight of 25g, and completes a cardiac cycle in 0.9 secs which is 250-660 bits/mins, with a stroke volume of 20-46 mu. Some of the materials used in the previous study in the construction of cardiac phantom include PVA cryogel, latex, silicone gel, and balloon **Jordi L. Tremodela, et al(2012)**.

2. Theoretical background

Magnetic resonance imaging deals with the interaction of certain atomic nuclei in the body with an external magnetic field. The hydrogen atom is good for MRI since it is abundant in the human body in large quantities, most of it in water molecules, and is a single proton. Hydrogen nucleus spin is $I=1/2$, which generates angular momentum p , along the spin axis given by equation (1), **Vaughan, et al, (2004)**

$$p = \hbar I \quad (1)$$

Where \hbar is Planck's constant/ 2π .

B_0 is the symbol for the main magnetic field and is measured in Tesla (T) typical value range from 1.0 T to 3.0 T in clinical MRI, while preclinical MRI uses an even higher magnetic field of 4.7 T to 7 T. The quantum model of Nuclear Magnetic Resonance (NMR) states that only two orientations of the magnetic moment are allowed, in the presence of an applied magnetic field. The nuclear spin in an applied magnetic field has $2I + 1 = 2$ possible orientations (Since $I = 1/2$), either parallel or antiparallel to the direction of the field B_0 , and this corresponds with the two energy states low and high, and with energy difference ΔE , given by Equation 2, **Vaughan, et al, (2004)**.

$$\Delta E = \gamma \hbar B_0 \quad (2)$$

$$E = h\nu = \hbar\omega, \quad \hbar\omega = \Delta E = \gamma \hbar B_0$$

$$\omega = \gamma B_0 \quad (3)$$

where ω is the resonance frequency for proton and γ is the gyromagnetic ratio.

At thermal Equilibrium the spins are distributed between the high and lower energy levels, though there are more spins in the lower energy level than higher energy level. In a sample with large number of nuclei, the spins will align randomly between the high and lower energy levels. The equilibrium distribution between the higher and lower energy level is given by Boltzmann's Equation (4).

$$(N_L - N_H) / N_H = \hbar\omega / kT = \hbar\gamma B_0 / kT \quad (4)$$

Where N_L is the number of spins in the lower energy level and N_H the number of spins in the higher energy level, k is Boltzmann's constant and T absolute temperature.

Cardiac MR images are improved by the use of cardiac gating. During image acquisition, MR images suffer from motion artifacts caused by both cardiac and respiratory movement. But with modern imaging techniques, cardiac MR image qualities have improved by reducing the total time of image acquisition and by using cardiac and respiratory gating. Cardiac MRI is used to obtain the anatomical image of the heart and vessels, for patients with cardiac diseases to check for abnormalities. These images could be obtained at different views conventionally (axial, coronal, or sagittal views), but other views are carried out for most cardiac studies (long axis, short axis, or views of valves). The heart is imaged repeatedly at a single slice throughout the cardiac cycle, data collection takes place over multiple cardiac cycles **Bartling, et al, (2010)**.

Cardiac gating is used for MRI data acquisition of the cardiac cycle, which begins at the detection of a physiological event (R-wave of ECG serves as the trigger), to obtain an image slice at a particular time in the cardiac cycle. A typical acquisition might use a 128 x 128 pixel image matrix, so 128 ECG triggers collecting 1 phase encoding step at the triggering point **Eze, et al, (2018)**.

3. Materials and methods

The materials used for this work are; a 300mm internal diameter superconducting magnet (Magnex UK) 4.7T preclinical MRI system, in the Biomedical Physics building, University of Aberdeen. Generates horizontal B_0 field, with actively shielded gradient coil (Magnex UK) internal diameter 220mm, driven by linear amplifiers (7796, AE Tecron, USA), a birdcage RF coil was used to transmit and receive signal at Larmor frequency.

In order to generate a realistic flow and motion in the phantom, an external control unit was used to drive a pump with constant frequency to produce a flow rate and motion similar to values found in-vivo. The phantom used to represent the heart chamber is entirely non-magnetic and is placed in center of the scanner. While the pump, solenoid valve and control electronics circuit are kept at a distance from the system for safety. The system is placed at 1m high to level with the magnet isocentre from the ground. This was done to have a constant pressure at both ends of phantom. The phantom is made of balloon filled with water connected via a nylon T-piece of 5m length of rigid PVC (polyvinyl chloride) tubing of internal diameter of 3mm, connected to a 12V water pump and solenoid valve located outside the 4.7T scanner.

The waveform generated was designed with three NE555 database multivibrators. NE555 are precision timing circuits that are capable of producing accurate oscillation or time delays, it can operate with supplies of 5V to 15V and are capable of sourcing current up to 200mA.

An astable multivibrator; was used to set the flow pulse frequency. The frequency and duty cycle of the flow switching can be controlled independently. It is used to control the frequency range of 3.5 – 5Hz or 210 beats per minute. Connecting two external resistors and a single external capacitor, the frequency, and the duty cycle can be controlled independently as shown in equation(5).

$$\text{Frequency} = 1.44 / (R_A + 2R_B)C \quad (5)$$

Where expected frequency = 3.5Hz, $R_A = 4.7K\Omega$, $R_B = 4.7K\Omega$, $C = 36\mu F$. The required capacitor is $36\mu F$, but the available capacitor is $33\mu F$, the output pin3 of the NE555 is connected to a monostable multivibrator.

Monostable multivibrators were used to generate a pulse, with a duration independent of the astable oscillation frequency. And is triggered via a high pass filter connected to the output pin with a cut-off frequency of 3.4KHz. And is also used to set a gating duration. A gating trigger is required to enable the MRI system to generate gated images that align with the cardiac cycle. The R-wave of an ECG is the trigger.

Pulse Width Modulation (PWM), was used to control the duty cycle output from the astable multi-vibration operation which is fed into the output of the monostable operation (pin2) clock input. The duty cycle is controlled by the resistor value of R_A and R_B

$$\text{Duty cycle (D)} = (R_A + R_B) / (R_A + 2 * R_B) \quad (6)$$

The output pin from NE555 monostable multivibrator is connected to an (IN4148 diode) which acts as a rectifier, and output from the diode to the resistors in series and to (2TX653)NPN power transistor which drives the solenoid valve. The transistor is connected in series with a current limiting resistor to a 12V voltage supply to control the solenoid valve, as shown in Figure 1.

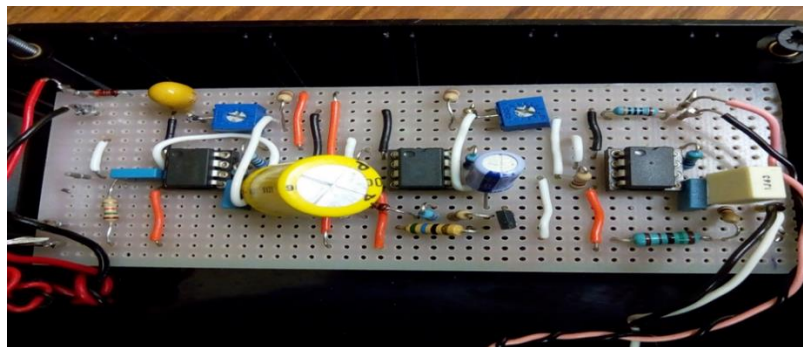


Figure 1 Flow control board

The solenoid valve is controlled using a power transistor switching by multivibrator circuits which also generate a gating pulse to stimulate an R-wave trigger for gated MRI acquisitions.

The flow control circuits were soldered into fiber-glass strip-board as shown in Figure 1, for the three multivibrators with a power supply of 12 V from an external source. A diode is connected in series in the positive (+Ve) row to prevent reverse polarity and also a $220 \mu F$ capacitor between the power supply rows to limit motor noise.

3.1. The Flow Phantom Design (circulating system)

The balloon part of the phantom was fixed on the 4.7 T MRI system's animal bed, as shown in Figure 3, directly over a 30mm diameter surface coil normally used to image the rat heart. The flow system was primed with water to mimic blood and the bed was loaded into the MRI magnet for imaging.

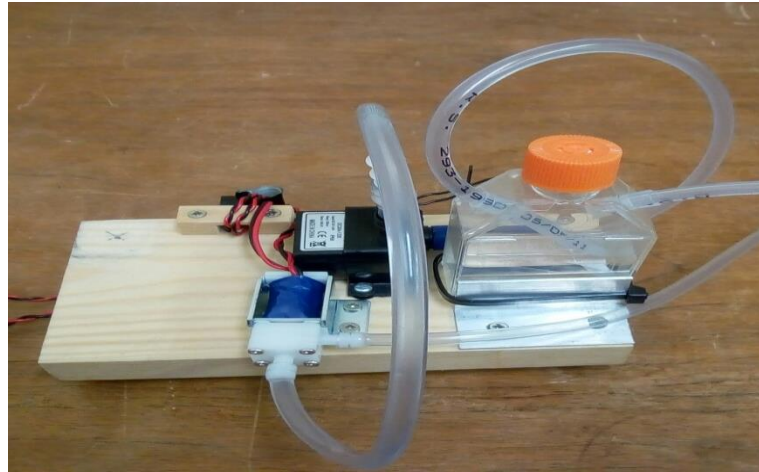


Figure 2 Pump, solenoid valve, and water reservoir.

The heart chamber is modeled by a small rubber balloon fed with a pulsed water flow controlled by a solenoid valve and timing circuit.

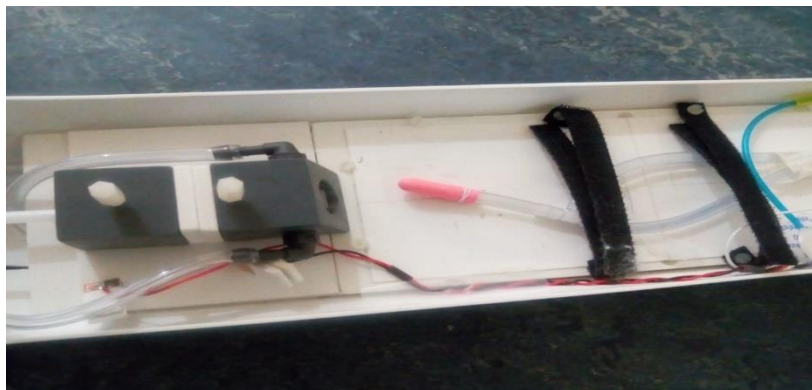


Figure 3 The heart chamber phantom mounted on the animal bed over a surface coil.

4. Results

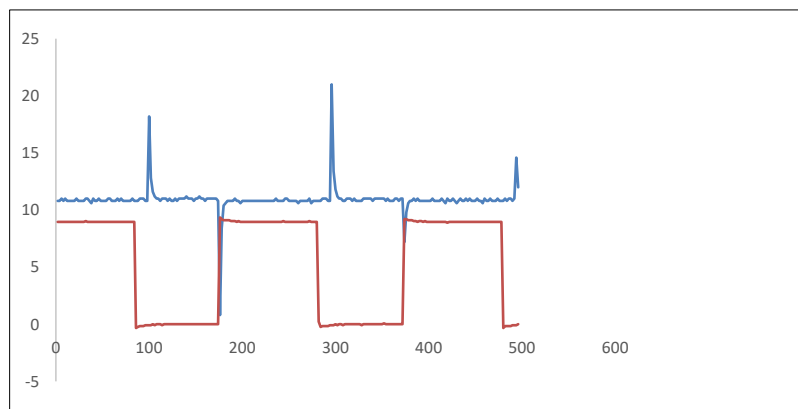


Figure 4 Output pulse from the astable multivibrator used to control the overall pulse rate (grey) and the high pass filtered output used to trigger subsequent monostable multivibrator stages (orange).

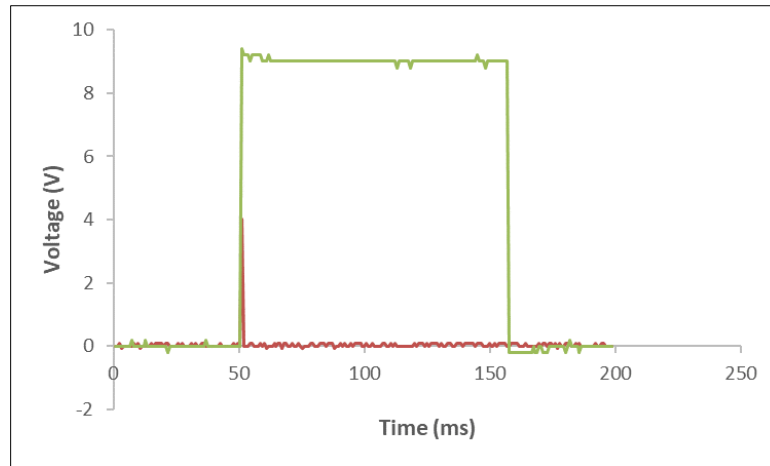


Figure 5 Output from monostable multivibrator use to control the solenoid valve drive (grey) and potential divider output used for MRI trigger (orange)

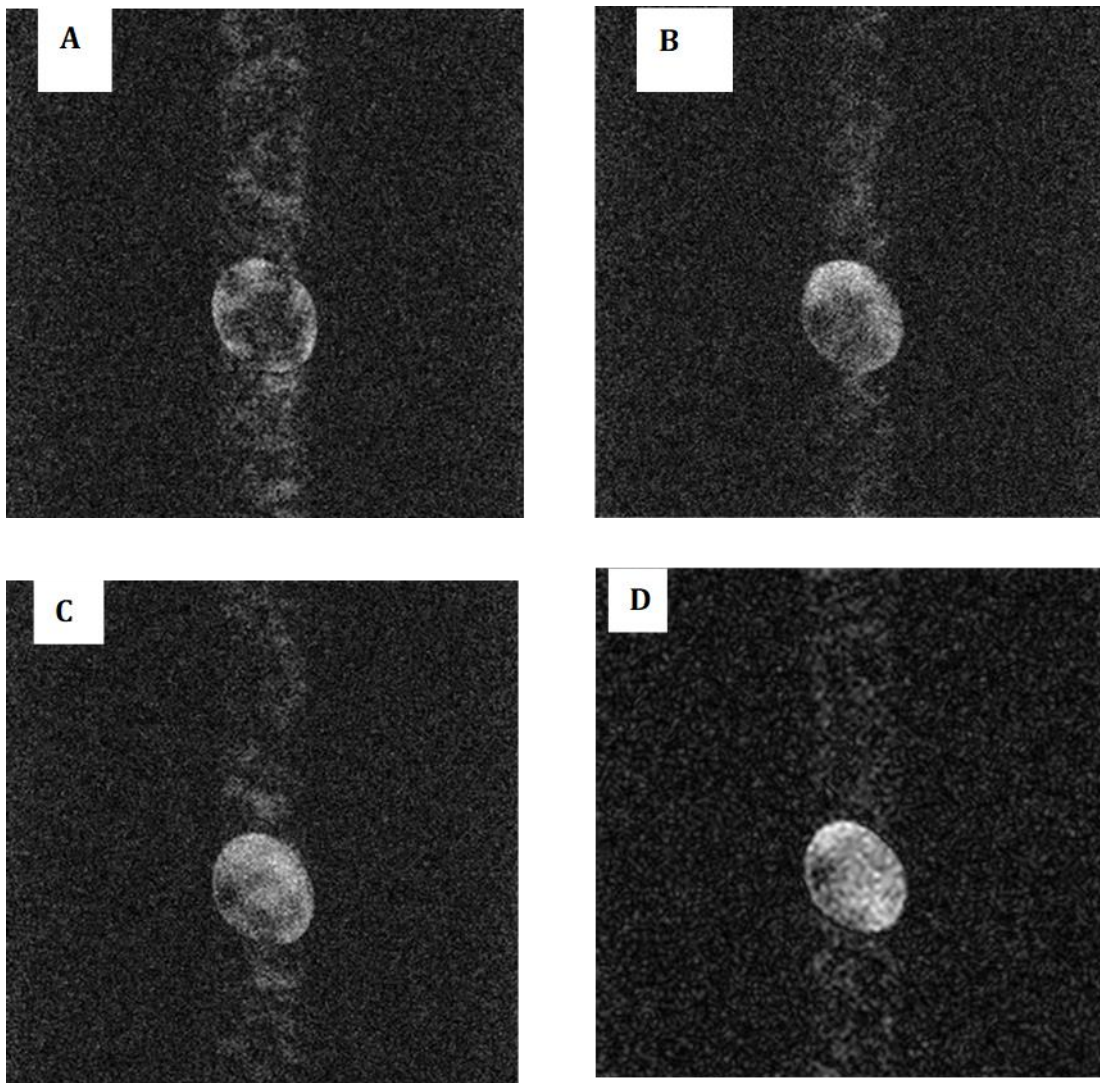


Figure 6 Gradient echo MRI scans of cardiac phantom acquired with transmit receive volume coil.

5. Discussion

Because of its ability to readily control the characteristics of the balloon, silicone gel was chosen for this work, its elastic modulus, and relaxation time of T_1 and T_2 . The cardiac phantom as shown in Figure 2 above is made of a balloon filled with water connected through a nylon T-piece to two 5m lengths of rigid pvc tubing of 3mm internal diameter to a 12V water pump and solenoid valve located outside the 4.7T scanner.

The flow is switched on and off with the solenoid valve to cause the balloon to pulse as the pressure changes, simulating a beating heart chamber. The solenoid valve is controlled using a power transistor switching by multivibrator circuits which also generate a gating pulse to simulate an R-wave trigger for gating MRI acquisition.

Figure 4, is a voltage-time plot acquired with a digital storage oscilloscope (72-8395, Tenma, China) of the astable multivibrator output used to set the pulse rate in the phantom. The direct output, shown in orange has a period of approximately 200 ms, corresponding to a pulse rate of 5 Hz or 300 bpm. The high pass filtered output shown in blue is used to trigger the monostable pulse generators which drive the solenoid valve and MRI gating input. Figure 5 shows voltage-time plots of the trigger pulses from two monostable circuits acquired with a digital storage oscilloscope (72-8395, Tenma, China). The gray trace shows the output of the monostable used to control the solenoid valve drive, here, set for a pulse width of approximately 110 ms, and the orange trace shows the output of the MRI trigger monostable, with a width of approximately 0.57 ms and after attenuation by the potential divider of 4V.

From Figure 6 (A) image with motion, echo time (TE) = 15 mm shows artifacts along the phase encoding direction. (B) with motion and gating, TE = 15 mm. (C) acquired with motion and gating, and (D) acquired with reduced echo time TE = 11 mm. All images used repetition time (TR) = 200 ms, slice thickness 1 mm, the field of view FOV = 40 mm, 256 x 256 pixels, and bandwidth 50kHz.

Images acquired with reduced TE = 11 mm, (D) has useful SNR and reduced artifact compared to (C) with TE = 15 mm, same TR = 200 ms, and FOV = 40 mm.

The second set of images was acquired with surface coils since images in Figure 6A-D appear with much noise in the background signal and images in Figure 7 appear with reduced noise.

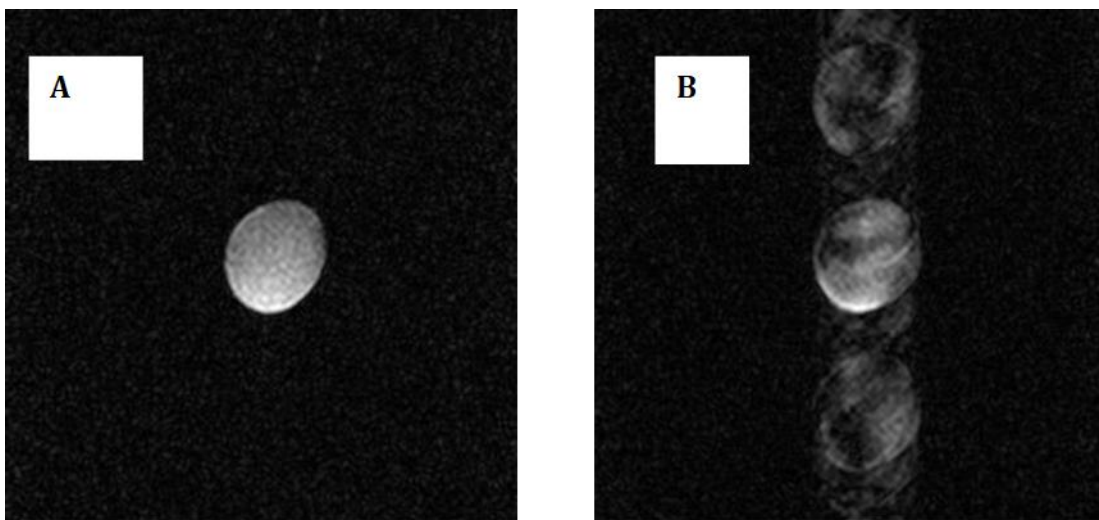


Figure 7 Gradient echo MRI scans of the cardiac phantom acquired with the surface coil

Figure 7 shows an image acquired with a surface coil with a higher signal-to-noise ratio (SNR), image (A) was acquired without motion, and image (B) was acquired with motion but introduces ghosting artifacts in the phase encoding direction. Slice thickness = 1, field of view (FOV) = 30mm, echo time (TE) = 10ms, repetition time (TR) = 500ms, matrix 256 x 256 pixel. Values of SNR measured at 4.7 T for images acquired with gradient echo MRI scan as shown in Figure 7, for A = 21170 ± 264 and B = 1251 ± 90 , these figures being the mean \pm standard deviation over the imaged signal.

6. Conclusion

The cardiac phantom has successfully been developed using a small balloon to represent a heart chamber and imaged in a 4.7T preclinical MRI scanner. Though, with high frequency, the pump makes a click sound and when the phantom is not at the same height as the control unit, there is a collapse in the pump cycle.

Images acquired with gradient echo pulse sequence with shorter TE of 5 ms and using surface coil displayed improved image contrast and have useful signal-to-noise ratio Fig7, compare to images acquired with birdcage coil which show ghosting artifact resulting from motion as seen in Figure 6a-d. Also has reduced image acquisition time and shows the myocardia movement through the image plane during the cardiac cycle.

In this research work, the cardiac phantom was imagined in air, but an improvement in this work would be, to place the phantom in a tube surrounded with water, to have a representative of the nuclear magnetic resonance (NMR) characteristic of a mouse myocardial function and its relaxation time (T_1 , T_2 values), and flow velocity in the phantom. Or the use of a thicker-walled material with properties closer to those of cardiac muscle, like PVA (polyvinyl alcohol) cryogel.

This research work used a variable resistor to adjust the frequency and duty cycle of the pump, this could be replaced to have a constant frequency and duty cycles to avoid the need of changing the operational cycle of the pump and have a constant output.

Compliance with ethical standards

Acknowledgments

We hereby acknowledge the Department of Biomedical Physics, University of Aberdeen, United Kingdom for using their resources for this work.

Disclosure of conflict of interest

All authors are in the same area of interest. Biomedical.

References

- [1] Bartling SH, Kuntz J, and Semmler W.(2010): Gating in small-animal cardio-thoracic CT. *Methods*, 50:42–49.
- [2] J-P. Vallee, M.K. Ivancevic, and D. Nguyen (2004). Status of Cardiac MRI in Small Animals. *Magnetic Resonance Materials in Physics, Biology, and Medicine*: 17, 149-159.
- [3] BH Brown (1999). *Medical Physics and Biomedical Engineering*; Institute of Physics Publishing Aberdeen UK.
- [4] Herrmann, K. H, Pfeiffer, and N. Krumbein I.(2014): MRI Compatible Small Animal Monitoring and System for whole body scanners, 24, 55-64.
- [5] . J cardiovasc gagn reson (2006). How to Perform an Accurate Assessment of Cardiac Function in Mice Using High-Resolution Magnetic Resonance Imaging. 8,693-701.
- [6] Steve Fortune, Maurits A. Janson,, Tom Anderson, Gillian A. Gary, Jurgen E. Schneider, Peter R. Hoskin, and Ian Marshal. (2012). Development and Characterization of Rodent Cardiac Phantoms: Comparison with in-vivo Cardiac Imaging. *Magnetic Resonance Imaging*. 30(8): 1186-1191
- [7] Vaughan, J.T., Adriany, G., Snyder, C.J., Tian, J. (2004). "Efficient high-frequency body coil for high-field MRI". *Magnetic Resonance in Medicine*. 52 (4): 851–859.
- [8] A.C.Riches, J.G.Sharp, D.Brynmor Thomas and Vaughan Smith (2009). Blood Volume Determination in Mouse. *J Physiol*. 228(2):279-284.
- [9] B.E. Eze, P.O. Ushie, K.B. Ndifon (2018). Physiological Monitoring for Preclinical Magnetic Resonance Imaging. *International Journal of Scientific & Engineering Research* 9(11), 1033-1038.
- [10] Jordi L Tremoleda, Angela Kerton, and Willy Gesell (2012). Anaesthesia and physiological monitoring during in vivo imaging of laboratory rodents: considerations on experimental outcomes and animal welfare. *EJNMMI Research*, 2:44.